Experimental tests on the optimal management of all-electric dwellings

Jacopo Vivian[1], Angelo Zarrella[1], Giorgio Besagni[2], Lorenzo Croci[2]
[1]Department of Industrial Engineering - University of Padova, Padova, Italy
[2]Ricerca Sistema Energetico S.p.A., Milano, Italy

Abstract

European policies are fostering the electrification of end uses including the space heating and cooling systems in order to decarbonise the housing stock. The deep penetration of electrical loads and domestic PV plants has therefore become an important topic for researchers and engineers working in the building sector. In this context, this paper presents a recently constructed laboratory for testing efficient management strategies in all-electric dwellings. The article describes the lab and the model predictive control strategy developed to minimize economic costs for space heating and cooling while guaranteeing thermal comfort in the indoor environment in presence of a simulated rooftop PV system. The proposed controller exploits prior knowledge about physical and geometrical properties of the building. The first tests, carried out in offline mode, demonstrated the effectiveness of this approach. The proposed Building Energy Management System (BEMS) exploits the flexibility offered both by the building structure and by the thermal storage tank to minimize costs in both the heating and cooling season. Future work will put other electrical devices under BEMS control.

Key Innovations

- Model Predictive Controller tested on-field
- Lumped-capacitance building models allow to exploit a-priori knowledge of the building
- Exploitation of combined flexibility from building structures and thermal storage tank
- A detailed model of the lab is under development for generalizing the results

Practical Implications

This article describes a new lab to test innovative strategies that improve the efficiency of buildings. We propose a technology that increases the self-consumption from rooftop PV systems with no need of batteries!

Introduction

It is widely accepted that the large-scale deployment of heat pumps is a promising way toward the decarbonisation of the heating sector. This trend will severely affect the power consumption patterns in the electrical distribution systems (Barton et al., 2013). At the same time, increasing penetration of small-scale renewable energy sources such as domestic *PV* systems is pushing the energy system towards a decentralised structure (Pierro et al., 2020). In such an energy transition, Building Energy Management Systems (BEMS) play a key role as they can shift energy consumption towards the most convenient time windows. BEMS may pursue individual objectives, such as cutting costs for single dwellers while guaranteeing a comfortable indoor environment (Vivian et al., 2020a) or system-level objectives, such as reducing the peak loads on electrical distribution grids (Vivian et al., 2020b) or providing services to the power grid (Romero Rodríguez et al., 2019). In both cases, the buildings could take advantage from different flexibility sources to decouple the supply-side and the demand-side, such as thermal energy storage systems or the inertia of building structures (Arteconi et al., 2016). Model Predictive Control (MPC) seems to overcome rule-based controllers based on simple heuristics to fully exploit the energy flexibility of building structures and thermal storage systems using heat pumps (Péan et al., 2019).

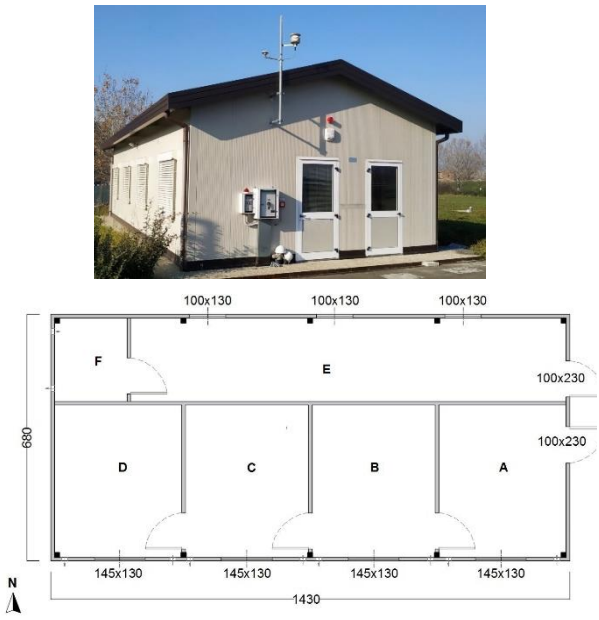

Figure 1. (a) Photo and (b) floor plan of the lab.

This paper contributes to the ongoing discussion and presents a laboratory developed by Ricerca Sistema Energetico in Piacenza (Italy). The goal of the laboratory is to simulate the performance of an all-electric residential building, to validate numerical approaches and to test novel, efficient and reliable system layouts and smart

control strategies. In particular, this article investigates the use of a well-known simplified building model to exploit a-priori knowledge of the building for control purposes. Secondly, the article presents the first experimental tests of a model predictive controller that is able to exploit the flexibility offered by both the building structure and the thermal storage tank in both heating and cooling season.

Lab description

The 100 m^2 internal surface laboratory shown in Fig.1 is equipped to simulate the performance of an efficient "all-electric" building. To this end, the laboratory has been equipped with (i) an air-to-water heat pump air conditioning system connected to four fan coils with a 300-liter water heat storage tank; (ii) a heat pump water heater with 200-liter storage tank for domestic hot water (DHW) production; (iii) an air/air conditioning system consisting of an outdoor condensing unit and four indoor units with a nominal cooling capacity of 6.8 kW; (iv) four air extractors; (v) a set of electrical appliances (e.g., washing machine, dryer, dishwasher and combined refrigerator). The HVAC system is illustrated in Fig. 2. In the upcoming months, the laboratory will be also equipped with a PV system with inverter and storage battery. In the meanwhile, the PV system has been simulated –see PV model section. A monitoring system allows to read data logged by the environmental sensors such as temperatures, mass flow rates, heat and power flow and automatically controls the system and communication with the heat pump. The software was created in the LabView environment based on a personal computer and on Advantech acquisition modules. The communication architecture uses Modbus ASCII and Modbus RTU fieldbuses on RS485 network. A preliminary analysis on the energy performance of the lab based on EnergyPlus simulations showed that the specific annual energy demands are approximately 68 kWh/m^2 for heating and 13 kWh/m^2 for cooling, including both sensible and latent loads. The whole analysis has not been included in this article to facilitate its readability.

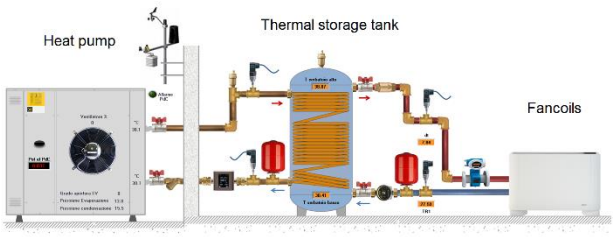

Figure 2. Synoptic panel of the HVAC system.

Models

Lumped capacitance building model

The lumped capacitance model used to reproduce the thermal behavior of the lab is the well-known 5R1C model proposed by Standard ISO 13790 (International Organization for Standardization, 2008). The Standard uses the electrical analogy and distributes the heat gains to three temperature nodes of an equivalent thermal network: Φ^{ia} to the indoor air temperature node (θ^i), Φ^{st} to the surface temperature node (θ^s) and Φ^m to the thermal mass temperature (θ^m) node. These heat gains derive from the sum of HVAC heat output Φ^{hc}, solar heat gains Φ^{sol} and internal heat gains Φ^{int}. The internal heat gains have been assumed equal to a constant heat flow rate $\Phi^{int,0}$. The indoor air temperature can then be found by solving the linear system given by the energy balance on the mentioned temperature nodes:

$$H_{ve}(\theta_t^{su} - \theta_t^i) + H_{tr,is}(\theta_t^s - \theta_t^i) + \Phi_t^{ia} + f_{conv}\,\Phi_t^{hc} = 0 \quad (1)$$

$$H_{tr,w}(\theta_t^e - \theta_t^s) + H_{tr,is}(\theta_t^i - \theta_t^s) + H_{tr,ms}(\theta_t^m - \theta_t^s) + \Phi_t^{st} + (1 - f_{conv})\,\Phi_t^{hc} = 0 \quad (2)$$

$$H_{tr,em}(\theta_t^e - \theta_t^m) + H_{tr,ms}(\theta_t^s - \theta_t^m) + \Phi_t^m = \frac{C_m}{\tau}(\theta_t^m - \theta_{t-\tau}^m) \quad (3)$$

where the capacitance term C_m represents the thermal inertia offered by the building structures. The other building parameters are the ventilation heat transfer coefficient H_{ve}, the coupling conductance between internal air and surface node $H_{tr,is}$, the thermal transmission coefficients of the windows $H_{tr,w}$ and of the opaque building components $H_{tr,op}$. The latter is divided into two components, $H_{tr,em}$ and $H_{tr,ms}$. The air supply temperature due to infiltration and/or ventilation (θ^{su}) is equal to the external air temperature (θ^e) in case there is no mechanical ventilation system and f_{conv} is a parameter that accounts for different radiative and convective contributions of HVAC terminals (example: f_{conv}= 1 for fancoils, f_{conv} = 0.5 for radiators). This model is able to accurately capture the thermal response of buildings especially in the heating season, whereas it is less accurate in the cooling season (Vivian et al., 2017). However, those results were obtained by calculating the parameters with analytical procedures. Instead, here the parameters are calculated with a data-driven calibration procedure as explained in the methodological Section.

Heat pump model

The simplified steady-state model adopted for the air source heat pump consists of three equations. The first equation correlates the heat pump capacity, i.e. the maximum thermal power output, to temperatures of the heat source (external air) and heat sink (thermal storage tank). In general, the polynomial law used for this correlation may be of the first, second or third order. Eq. (4) shows the polynomial of the second order. Eq. (5) assumes that the thermal power output is a fraction of the capacity equal to the ratio between the compressor speed n and the maximum speed n_{max}. Finally, Eq. (6) assumes that the power consumption of the heat pump including auxiliaries can be calculated based on a polynomial similar to Eq. (4), where COP is the coefficient of performance of the heat pump. In order to calculate $Q_{hp,max}$ and COP as a boundary condition for the optimization –see Methods Section-, θ_{hs} has been

replaced with the average supply temperature of the heat pump during the last 24 hours $\theta_{hp,out}$.

$$Q_{hp,max} = a_0 + a_1\,\theta_e + a_2\,\theta_{hs} + a_3\,{\theta_e}^2 + a_4\,{\theta_{hs}}^2 + a_5\,\theta_e\theta_{hs} \quad (4)$$

$$\Phi_{hp} = \frac{n}{n_{max}}\,Q_{hp,max} \quad (5)$$

$$COP = \frac{\Phi_{hp}}{w_{hp}} = b_0 + b_1\,\theta_e + b_2\,\theta_{hs} + b_3\,{\theta_e}^2 + b_4\,{\theta_{hs}}^2 + b_5\,\theta_e\theta_{hs} \quad (6)$$

PV system model

While the previous models were included among the constraints of the optimization problem, the photovoltaic system model replaces the real system, i.e. provides power production values depending on the forecasted solar radiation. The model used was taken from an open-source collaborative project called *pvlib* (F. Holmgren et al., 2018), which is based on the well-known clear sky model (Ineichen and Perez, 2002). The simulated PV system is assumed to be positioned on the south-oriented side of the roof, with a tilt angle of 20°. It consists of 8 modules with a nominal power of 220 W.

Methods

BEMS architecture

The Building Energy Management System (BEMS) was developed in Python with the logic of object oriented programming. It consists of several processes that are cyclically run on the computer of the lab where all measurements are collected. These processes include: (i) reading measurements from the plant and environmental sensors; (ii) reading weather forecast and update PV production forecasts accordingly; (iii) calibrating parameters of the lumped capacitance model; (iv) scheduling the heat pump operation for next hours. In its final version, the BEMS will perform these operations sequentially with a given frequency. This paper presents the current version where all operations are manually launched at the same time and the results of the main processes (calibration and optimization) is commented. As Fig. 3 shows, the BEMS relies on a model predictive control loop. Measurements of indoor and outdoor temperature, solar radiation and heat flow rate released from the HVAC plants to the indoor environment are stored in a history database. All these measurements are used to calibrate a lumped capacitance building model described in the Models Section. The calibration process carried out to find the parameters of the building model is described in the Methods section. Instead, the calibration of the heat pump model consists in the calculation of the coefficients of polynomials $a_1..a_N$ and $b_1..b_N$ –see Eq. (4) and (6)) through a linear regression. Once the optimal parameters are found through these calibration procedure, they are used to build the constraints of an optimization problem described hereafter. The optimization is the BEMS core, and relies on weather forecasts that are updated by an external service twice a day.

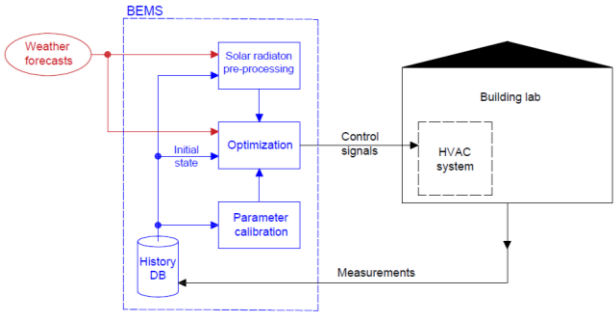

Figure 3. Qualitative scheme illustrating the BEMS architecture.

Calibration of the building model

The calibration is the numerical process by which the parameters describing the building's dynamic thermal behaviour in Eq. (1-3) are initially determined based on an approximate knowledge of the building physical and geometrical properties, and then iteratively recalculated to ensure that the lumped capacitance model described above adheres as much as possible to the real behaviour of the building. This operation is carried out by an optimisation algorithm that minimises the mean square error between the average indoor air temperature profile measured in the lab and the indoor air temperature calculated by the mentioned model. Thus, the objective function is:

$$\min_{x \in X} \sqrt{\frac{\sum_{t=1}^{T}(\theta_t^i(x) - \theta_t^{i,meas})^2}{T}} \quad (7)$$

where x = [C_m, $H_{tr,em}$, $H_{tr,is}$, $H_{tr,ms}$, $H_{tr,w}$, H_{ve}, f_{conv}, $\Phi^{int,0}$] is the optimal set of parameters that must be determined. The algorithm used to find the optimal set of parameters is called Particle Swarm Optimization (PSO), a nature-inspired optimization algorithm that does not make any assumptions about the problem and allow the exploration of very wide spaces of solutions (Kennedy and Eberhart, 1995). These algorithms have the advantage of always converging towards a solution and being insensitive to local minima, although being slower than classical gradient descent methods. At each iteration, the algorithm evaluates the objective function expressed in Eq. (4) at a number of points in the domain. Depending on the result obtained, the position of each point is updated in the next iteration according to a criterion inspired by the dynamics of swarms in the animal world. Each of these points, which represent the particles of the swarm, move in the domain as the number of iterations advances. This shift, represented by the velocity of the *i-th* particle in the Eq. (8), is determined by the superposition of three kinetic components: (i) an inertial component derived by the velocity at the previous iteration; (ii) a cognitive component where the particles keep memory of their best position (personal best) and therefore move in that direction; (iii) a social component where the particles move towards the best position reached by the entire swarm (global best). In Eq. (9) the position at the *k-th* iteration is updated according to the velocity calculated as described above.

$$v_i^{k+1} = w\, v_i^k + c_1\, r\left(p_{pb,i}^k - x_i^k\right) + c_2\, r\left(p_{gb,i}^k - x_i^k\right) \quad (8)$$

$$x_i^{k+1} = x_i^k + v_i^{k+1} \quad (9)$$

The parameters w, c_1 and c_2 represent the weight of the inertial, cognitive and social components of the algorithm, respectively. These parameters must be set according to the problem to be analysed and therefore need an initial sensitivity study to make the algorithm converge towards an optimal value in a reasonable time. The value r is a random number between 0 and 1 and must be calculated at each iteration for each particle. This random variable makes the algorithm stochastic, i.e. based on a random exploration of the domain by the swarm that resembles a natural process. The greater is the cognitive component compared to the social one, the greater is the propensity of the algorithm to explore the domain.

Optimization problem

The current version of the BEMS controls only the heat pump and the circulation pump of the secondary water loop (see Fig. 2). In the future, also the DHW boiler and other electrical devices will be integrated within the BEMS. The core of the BEMS is a *mixed integer linear programming* (MILP) problem solved in a rolling horizon scheme. This means that the optimization is repeated with a predetermined sample time. At each step, the operation of the HVAC system is planned for the next H hours, where H is the horizon of the optimization problem. The planning consists in determining the circulation pump on the water loop of the fancoils and the state of the heat pump, which consists of an on/off signal and a frequency signal communicated to the inverter-driven compressor. The optimization problem consists in the minimization of the economic objective function:

$$\min_{\Xi} \sum_t (\lambda_t^b w_t^b - \lambda_t^s w_t^s) + \sum_t \gamma\left(\delta_t^{\uparrow} + \delta_t^{\downarrow}\right) \quad (10)$$

Subject to the constraints in Eq. (1-3) and those listed in the following:

$$w_t^b + w_t^{pv} = w_t^s + w_t^{hp} + w_t^{od} \quad (11)$$

$$\theta_t^{i,min} - \delta_t^{\downarrow} \le \theta_t^i \quad (12)$$

$$\theta_t^i \le \theta_t^{i,max} + \delta_t^{\uparrow} \quad (13)$$

$$\Phi_t^{hp} - \Phi_t^{hc} - UA(\theta_t^{hs} - \theta_t^i) = \frac{\rho\, V_{hs} c_p}{\tau}\left(\theta_t^{hs} - \theta_{t-\tau}^{hs}\right) \quad (14)$$

$$\theta_H^{hs} \ge \theta_0^{hs} \quad (15)$$

$$\Phi_t^{hp} = r_{min} Q_t^{hp,max}\, u_t^{hp} + Q_t^{hp,mod} \quad (16)$$

$$Q_t^{hp,mod} \le u_t^{hp}\,(1 - r_{min})\, Q_t^{hp,max} \quad (17)$$

$$\Phi_t^{hp} = COP_t\, w_t^{hp} \quad (18)$$

$$x_t^{su} \ge u_t^{hp} - u_{t-\tau}^{hp} \quad (19)$$

$$x_t^{su} \le u_t^{hp} \quad (20)$$

$$\Phi_t^{hp} \ge x_t^{su}\, r_{min,start}\, Q_t^{hp,max} \quad (21)$$

$$\Phi_t^{hc} = r_{min,fc} Q_t^{hc,nom}\, u_t^{hc} + Q_t^{hc,mod} \quad (22)$$

$$Q_t^{hc,mod} \le u_t^{hc}\left(1 - r_{min,fc}\right) Q_t^{hc,nom} \quad (23)$$

$$\Phi_t^{hc} \le k_{fc,H}\left(\theta_t^{hs} - \theta_t^i\right) \quad (24)$$

where λ_t^b and λ_t^s are the purchase and sale price of electricity; w_t^b and w_t^s represent the amount of electricity bought by and sold to the grid, and the second sum is a penalty that aims at limiting the events in which the air temperature goes beyond the boundaries of thermal comfort. The temperature difference between the indoor air temperature and the upper/lower thermal comfort bound is defined by variables $\delta_t^{\uparrow}$ and $\delta_t^{\downarrow}$, respectively. Further details about the optimization can be found in an early version of this work (Vivian and Mazzi, 2019). Eq. (11) represents the electrical energy balance at building level; Eq. (12-13) define the boundaries of indoor thermal comfort based on the temperature setpoints fixed by the user; Eq. (14) is the thermal energy balance of the hot water tank and Eq. (15) imposes that the temperature of the water in the tank at the end of the horizon must be at least equal to its initial temperature. This choice was made to avoid continuous discharging to pursue cost minimization. Eq. (16-18) describe the heat pump performance; Eq. (19-21) set the minimum power during the heat pump start-up; Eq. (22-24) set the minimum heat flow rate exchanged by the heat emitters and the maximum one as a function of the temperature of the water coming from the tank. The whole set of constraints includes 7 equations and 12 inequalities that must be repeated for each step t in the horizon, i.e. $\forall t \in [1, H]$. There are 16 unknown variables at each step: u_t^{hc}, u_t^{hp}, Φ_t^{hc}, Φ_t^{hp}, θ_t^{hs}, θ_t^i, θ_t^s, θ_t^m, w_t^{hp}, w_t^s, w_t^b, x_t^{su}, $Q_t^{hp,mod}$, $Q_t^{hc,mod}$, $\delta_t^{\downarrow}$ and $\delta_t^{\uparrow}$. Therefore, considering a 24-hours-horizon with 15-minutes-steps leads to an optimization problem with 8·96 = 768 equalities, 8·96 +1= 769 inequalities and 16·96 = 1536 unknown variables. Therefore, the problem has (16-8)·96 = 768 degrees of freedom.

Results

Calibration of the heat pump model

In order to find the coefficients of the polynomial functions, a linear regression has been implemented selecting only data corresponding to inverter frequencies greater than 59.5 Hz (the maximum frequency being 60 Hz). The square points in Fig. 4 represent the thermal power and the COP as a function of external air temperature and of the average thermal storage temperature. The coloured area in the graphs represents the second-order polynomial curve obtained by the regression to approximate the data cloud. As Fig. 4 shows, the correlation coefficient R^2 is 86% for the heat pump capacity and 63% for the COP. The lower correlation index can be explained by the fact that the COP considers two phenomena with different dynamics: while the electrical power absorbed by the compressor has an almost instantaneous response considering a sampling time of one minute, the thermal power approaches its

steady-state value more slowly. These transients occur mainly during compressor start-up periods. In these moments, COPs are typically lower than during steady-state operation.

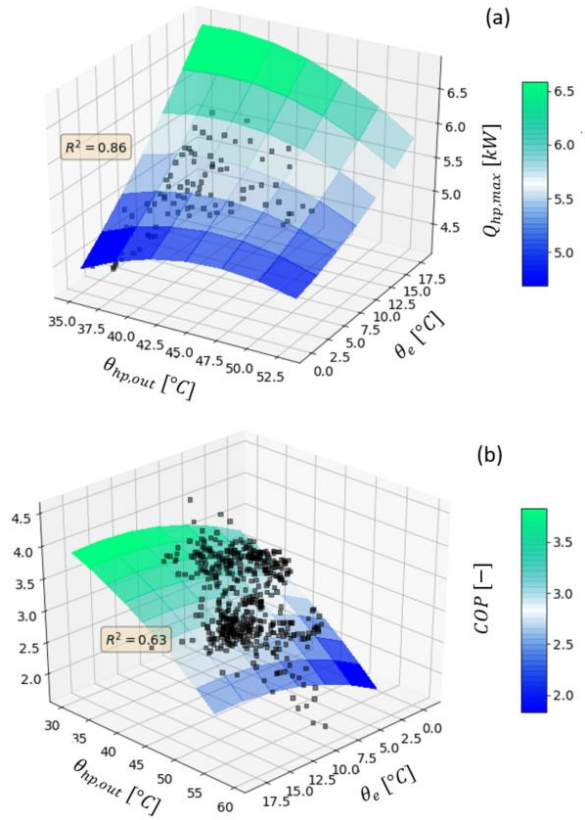

Figure 4 a) Capacity and (b) COP of the heat pump: measurements vs linear regression model.

Calibration of the building model

Figure 5 shows the profile of the indoor air temperature obtained with the nominal parameters, i.e. thanks to the prior knowledge of the building (blue line), the profile obtained with the calibrated parameters (orange line) and the profile of the average temperature measured in the four rooms of the lab (dashed black line). The calibration includes three training days (from 17/12/20 at 10:45 to 20/12/20 at 10:45) and one testing day (from 20/12/20 to 21/12/20). The profile obtained from the nominal parameters shows a similar trend compared to the measured temperature profile. However, there is a gap between the two and the indoor temperature peaks due to the intermittent behaviour of the fancoils are higher than those measured in the lab. The calibration process based on Particle Swarm Optimization is able to narrow these differences, bringing the model output closer to the measured one. In the chosen days, the RMSE between the profiles goes from 2.03 K (model with nominal parameters) to 0.59 K (model with calibrated parameters) during the training period. In the testing period, i.e. on the fourth day shown in the graph below, the RMSE reaches 0.89 K, which is probably linked to a change in the boundary conditions. Similar results have been obtained in the cooling period.

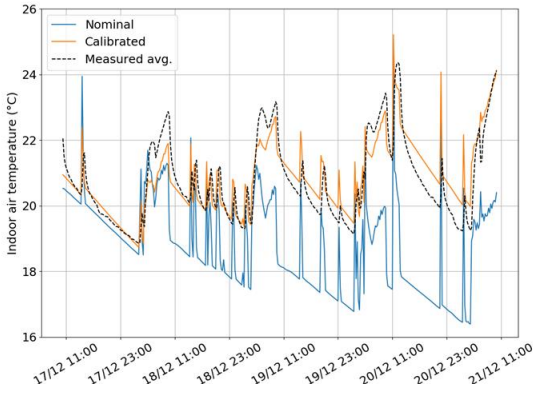

Figure 5 Example of building model calibration during the winter period.

Optimization results

Figure 6 shows the result of the optimisation performed in the laboratory at 1 am on 30/11/20 with a 24-hour horizon. The wide comfort range considered (21±2°C) was set to better appreciate the energy flexibility offered by the building structures and by the HVAC system. After an initial transient that brings the indoor air temperature (continuous blue line) from the initial state (approx. 23°C) to the minimum of the comfort band (19°C), the temperature remains at the minimum level throughout the day except when it is possible to self-produce energy with the PV system. In fact, when the simulated photovoltaic panels produce electricity (yellow line), the heat pump produces heat and charges the tank. The possibility of modulating the thermal output of the heat pump adapts its electrical consumption (black line) to the forecasted production of the PV modules.

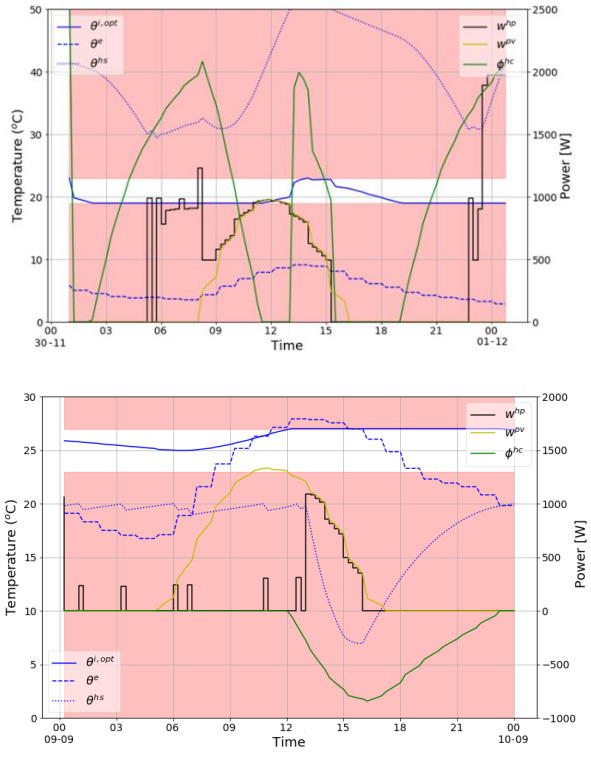

Figure 6. Optimization results during (a) a winter day and (b) a summer day.

The heat produced during these hours (from about 8 am to 3 pm) is not discharged directly into the room, but charges the thermal storage tank. The latter releases heat to the room both during the night and early morning hours due to the low outdoor temperature (blue dotted line), and from 1 pm onwards, when the tank has reached the maximum limit temperature and must therefore be discharged. This strategy can be appreciated by observing the green line, which represents the power profile transferred to the environment by the fan coils. This solution found by the optimiser takes maximum advantage of the combined inertia offered by the building structures and by the HVAC system. The state of charge of the tank, i.e. its average temperature θ_t^{hs} (blue dotted line) oscillates between a minimum and a maximum. In the summer season, the situation is mirrored: the internal temperature predicted by the optimiser is equal to the maximum allowed, except when the thermal storage can supply cold water that was produced at low cost by means of the photovoltaic system. During the night and in the morning, the external air temperature is lower than the internal one. Therefore, the heat pump only shows limited start-ups to maintain the water temperature in the tank below the maximum value allowed (20°C). During the first afternoon hours, the heat pump exploits the electrical energy produced locally by the PV system to cool down the tank. The fancoil operation is scheduled from 12 am to 11 pm with a maximum cooling load occurring around 4 pm.

Optimal control of the HVAC system

The monitored values of temperature and energy in the lab do not exactly match those predicted by the optimal planning. The difference is mainly due to the simplifications assumed in the first-principle equations describing the thermal behaviour of the system and by the inaccuracy of weather forecasts. Figure 7 shows, by way of example, the planned and realised behaviour during a test carried out on January 18th, 2021, where dashed lines represent the predicted optimal behaviour and dotted lines stand for the actual behaviour measured in the lab. The blue lines in Figure 7(a) show the predicted and measured outdoor air temperature. During the first hours, the measured temperature corresponds to the forecasted one, but from approximately 8 am it deviates with consequent underestimation of the heat losses due transmission and ventilation. The profiles of forecasted and actual water temperature in the tank show a diverging trend in the late morning. This can be explained by observing the heat exchange rate at the heat pump condenser –red lines in Fig. 7(b). Despite an overall similar trend on a daily basis, the spike occurring around 10 am reaches negative values, which means that the tank switches its role from heat sink to heat source in order to perform a defrosting cycle. As a result, the water temperature in the tank drops compared to the predicted optimal trend shown by the dashed green line in Fig. 7(a). As far as the secondary side of the HVAC system is concerned, the measured and optimal heat flow rate supplied by the fancoils (Φ^{hc}) also show a similar trend on a daily basis. However, the peak due to the start-up transient is underestimated by the linear model. The electrical demand of the heat pump –green lines in Fig. 7(b)- and the average indoor air temperature -black lines in Fig. 7(a)-, which are the most important variables for the optimization pursued by the BEMS, show a good match with the optimal values, which confirms the robustness of the proposed model predictive controller.

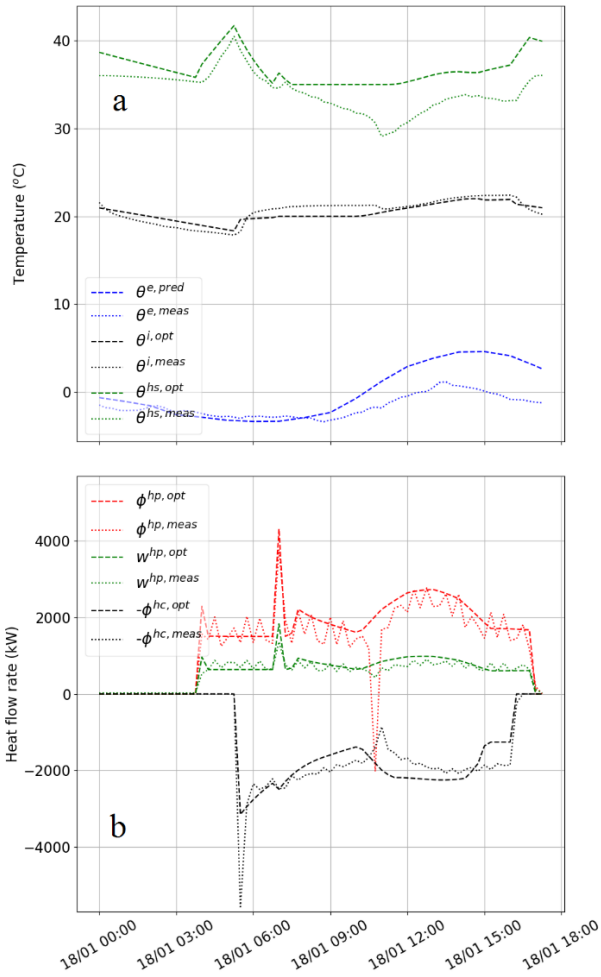

Figure 7. Optimal planning vs measured behaviour: (a) temperatures and (b) heat flow rates.

Conclusions

This article presents the first tests carried out in an experimental laboratory equipped with electrical devices including an air source heat pump for space heating and cooling. A model predictive control strategy was developed in order to minimize economic costs and indoor thermal discomfort. The underlying building model is based on the well-known simple hourly method of ISO 13790 Standard, where the heat transfer coefficients are first guessed based on physical and geometrical knowledge of the building and then calibrated using Particle Swarm Optimization. The short number of training days needed in the calibration process confirms the effectiveness of the proposed method. The optimization, carried out in offline mode, shows that the proposed strategy is able to maximize the self-consumption from the PV panel and to take advantage

from the flexibility offered by the combination of building structure and thermal storage tank in both the heating and cooling season. The first tests where the optimal planning is used to control the HVAC system show that the actual behaviour is slightly different from the predicted one due to inaccurate forecasts, simplifications introduced by linear constraints and due to the presence of defrosting cycles.

Potential contribution for future research

Future work will focus on the implementation of the presented Model Predictive Controller in online mode using a rolling horizon scheme. New electrical devices will be considered in order to improve the capability of the Building Energy Management System for all-electric dwellings. Indeed, this research is focused on the optimal management of energy flows in buildings under high electrification scenarios.

Although this paper is mainly focused on control aspects, the laboratory will also be of interest for the building simulation community. In fact, current activities include the development of a detailed dynamic model of the lab to be validated using measured data of indoor environmental conditions and thermal loads. The detailed dynamic model will be the basis of a digital twin used to test the optimal control strategies presented here (or other ones) on buildings with different physical characteristics, thus generalizing the results concerning the flexibility offered by building structures to all-electric dwellings.

Acknowledgements

The Authors would like to thank Nicolò Mazzi for his contribution in the preliminary phase of this work, and in particular for the formulation of the optimization problem.

References

Arteconi, A., Patteeuw, D., Bruninx, K., Delarue, E., D'haeseleer, W., Helsen, L., 2016. Active demand response with electric heating systems: Impact of market penetration. Applied Energy 177, 636–648. https://doi.org/10.1016/j.apenergy.2016.05.146

Barton, J., Huang, S., Infield, D., Leach, M., Ogunkunle, D., Torriti, J., Thomson, M., 2013. The evolution of electricity demand and the role for demand side participation, in buildings and transport. Energy Policy 52, 85–102. https://doi.org/10.1016/j.enpol.2012.08.040

F. Holmgren, W., W. Hansen, C., A. Mikofski, M., 2018. pvlib python: a python package for modeling solar energy systems. Journal of Open Source Software 3, 884. https://doi.org/10.21105/joss.00884

Ineichen, P., Perez, R., 2002. A new airmass independent formulation for the Linke turbidity coefficient. Solar Energy 73, 151–157. https://doi.org/10.1016/S0038-092X(02)00045-2

International Organization for Standardization, 2008. ISO 13790: Energy performance of buildings: calculation of energy use for space heating and cooling.

Kennedy, J., Eberhart, R., 1995. Particle swarm optimization, in: Proceedings of ICNN'95 - International Conference on Neural Networks. Presented at the ICNN'95 - International Conference on Neural Networks, IEEE, Perth, WA, Australia, pp. 1942–1948. https://doi.org/10.1109/ICNN.1995.488968

Péan, T.Q., Salom, J., Costa-Castelló, R., 2019. Review of control strategies for improving the energy flexibility provided by heat pump systems in buildings. Journal of Process Control 74, 35–49. https://doi.org/10.1016/j.jprocont.2018.03.006

Pierro, M., Perez, R., Perez, M., Moser, D., Cornaro, C., 2020. Italian protocol for massive solar integration: Imbalance mitigation strategies. Renewable Energy 153, 725–739. https://doi.org/10.1016/j.renene.2020.01.145

Romero Rodríguez, L., Brennenstuhl, M., Yadack, M., Boch, P., Eicker, U., 2019. Heuristic optimization of clusters of heat pumps: A simulation and case study of residential frequency reserve. Applied Energy 233–234, 943–958. https://doi.org/10.1016/j.apenergy.2018.09.103

Vivian, J., Chiodarelli, U., Emmi, G., Zarrella, A., 2020a. A sensitivity analysis on the heating and cooling energy flexibility of residential buildings. Sustainable Cities and Society 52, 101815. https://doi.org/10.1016/j.scs.2019.101815

Vivian, J., Mazzi, N., 2019. An algorithm for the optimal management of air-source heat pumps and PV systems. Journal of Physics: Conference Series 1343, 012069. https://doi.org/10.1088/1742-6596/1343/1/012069

Vivian, J., Prataviera, E., Cunsolo, F., Pau, M., 2020b. Demand Side Management of a pool of air source heat pumps for space heating and domestic hot water production in a residential district. Energy Conversion and Management 225, 113457. https://doi.org/10.1016/j.enconman.2020.113457

Vivian, J., Zarrella, A., Emmi, G., Carli, M.D., 2017. An evaluation of the suitability of lumped-capacitance models in calculating energy needs and thermal behaviour of buildings. Energy and Buildings 150, 447–465. https://doi.org/10.1016/j.enbuild.2017.06.021